From Vanadium Naphthalene (Vn−1Npn) Sandwich Clusters to VNp Sandwich Nanowire: Structural, Energetic, Electronic, and Magnetic Properties

ARTICLE *in* THE JOURNAL OF PHYSICAL CHEMISTRY A · FEBRUARY 2012

Impact Factor: 2.69 · DOI: 10.1021/jp2099398 · Source: PubMed

3 AUTHORS:

Yafei Li
Nanjing Normal University
48 PUBLICATIONS **2,046** CITATIONS
SEE PROFILE

Zhen Zhou
Nankai University
212 PUBLICATIONS **6,981** CITATIONS
SEE PROFILE

Zhongfang Chen
University of Puerto Rico at Rio Piedras
221 PUBLICATIONS **8,037** CITATIONS
SEE PROFILE

THE JOURNAL OF PHYSICAL CHEMISTRY A

Article

pubs.acs.org/JPCA

From Vanadium Naphthalene ($V_{n-1}Np_n$) Sandwich Clusters to VNp Sandwich Nanowire: Structural, Energetic, Electronic, and Magnetic Properties

Yafei Li,[†,‡] Zhen Zhou,*[,‡] and Zhongfang Chen*[,†]

[†]Department of Chemistry, Institute for Functional Nanomaterials, University of Puerto Rico, Rio Piedras Campus, San Juan 00931, Puerto Rico

[‡]Institute of New Energy Material Chemistry, Key Laboratory of Advanced Energy Materials Chemistry (Ministry of Education), Computational Center for Molecular Science, Nankai University, Tianjin 300071, P. R. China

Supporting Information

ABSTRACT: The structural, energetic, electronic, and magnetic properties of a series of vanadium naphthalene ($V_{n-1}Np_n$) sandwich clusters (SWCs) and the VNp sandwich nanowire (SWN) were investigated by means of density functional theory computations. In the energetically most preferred configuration of each $V_{n-1}Np_n$ SWC and SWN, the two nearest-neighbor Np rings form a 45° rotation angle, the two second-nearest-neighbor Np rings are parallel to each other, and V atoms align in a zigzag chain. The local magnetic moments in $V_{n-1}Np_n$ SWCs favor antiferromagnetic coupling due to the superexchange mechanism. Especially, both electron and hole injection can switch $V_{n-1}Np_n$ SWCs and VNp SWN from the antiferromagnetic state to the ferromagnetic state, thus manipulating the magnetization direction. These results suggest the potential applications of $V_{n-1}Np_n$ SWCs and VNp SWN in spintronics.

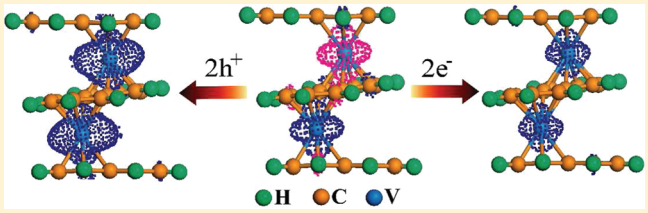

1. INTRODUCTION

Since the discovery of ferrocene [$Fe(C_5H_5)_2$] in the 1950s,[1] the sandwich clusters (SWCs) not only have greatly enriched the basic science of organometallic chemistry but also have found many practical applications, in catalysis, magnetic and optical materials, polymers, and molecular recognition, etc.[2] With the advancement of experimental techniques, in recent years many multidecked SWCs, including TM_nCp_m (TM = transition metals, Cp = cyclopentadienyl or C_5H_5), TM_nBz_m (Bz = benzene or C_6H_6), and $TM_n(COT)_m$ (COT = cyclootetatrene or C_8H_8), have been synthesized.[3−18] The structural, electronic, magnetic, and transport properties of these multidecked SWCs and the infinite one-dimensional (1D) sandwich nanowires (SWNs) have been extensively investigated theoretically.[19−51]

Many intriguing results have been reported so far. Among others, the structural properties of TM_nBz_m SWCs strongly depend on the character of the metal: early TM species (Sc, V, and Ti) prefer the linearly multidecked sandwich structure, whereas late TM (Fe, Co, and Ni) species tend to form the rice-ball structure (in which all the metal atoms are clustered at the center and surrounded by the benzene molecules).[3,5,27] Stern−Glelach deflection experiments[9,10] and density functional theory (DFT) computations both demonstrated that local magnetic moments of TM atoms could couple ferromagnetically in many SWCs,[23,24,26,34,36−38] which opens a new path to explore organic spintronics at nanoscale. Especially, DFT computations revealed that many 1D SWNs, such as TM-Bz,[30,32,35] TM-Cp,[36,37] hybrid TM-CpBz,[38,45,49,50] and TM-Ant (Ant = anthracene or $C_{14}H_{10}$),[38] can exhibit the intriguing half-metallicity (the coexistence of metallic nature for electrons with one spin orientation and insulating nature for electrons with the other), which is a key advantage for their application in spintronics.

Naphthalene (Np) is a well-known aromatic hydrocarbon molecule with a fused pair of benzene rings. Earlier experimental studies demonstrated that the Np molecule can capture transition metals (V, Ti, or Cr) to form sandwich complexes.[52−55] Remarkably, Kurikawa et al.[5] synthesized a series of multidecked V_mNp_n SWCs by using the laser vaporization method, and the observed $V_{2n-2}Np_n$ SWCs inspired Zhang et al.'s theoretical efforts to investigate the electronic and magnetic properties of 1D V_2Np SWNs.[43]

However, in the mass spectrum of V_mNp_n SWCs,[5] the peaks of these $V_{2n-2}Np_n$ SWCs, especially V_4Np_3 and V_6Np_4, are much less pronounced than those of $V_{n-1}Np_n$ SWCs, implying the higher abundance of $V_{n-1}Np_n$ SWCs. Since each Np ring can provide four sites on both sides of two η^6 rings, the formation of $V_{2n-2}Np_n$ SWCs is not surprising. However, why are so many $V_{n-1}Np_n$ SWCs with even higher abundance also synthesized during the reaction between V vapor and Np molecules? To our best knowledge, the electronic, magnetic, and even structural properties of $V_{n-1}Np_n$ SWCs have not been

Received: October 16, 2011
Revised: January 12, 2012
Published: January 17, 2012

studied. Addressing these issues will not only contribute to the basic knowledge of SWCs but also provide some insights for their promising applications.

In this work, we performed systematic spin-polarized DFT computations to investigate the structural, energetic, electronic, and magnetic properties of $V_{n-1}Np_n$ SWCs (n = 2−5) and its infinite 1D analogue, the VNp SWN. It is found that all the $V_{n-1}Np_n$ SWCs studied in this work follow the same growth pattern: the two nearest-neighbor Np rings form a 45° rotation angle, the two second-nearest-neighbor Np rings are parallel to each other, and the V atoms in $V_{n-1}Np_n$ SWCs align in a zigzag shape. $V_{n-1}Np_n$ SWCs have higher binding energies than the multidecked $V_{2n-2}Np_n$ SWCs. The local magnetic moments of $V_{n-1}Np_n$ SWCs and VNp SWN are antiferromagnetically coupled and can be tuned into ferromagnetic ordering through electron or hole injection.

2. COMPUTATIONAL DETAILS

Our spin-polarized first-principles DFT computations were performed by using a plane wave basis set with the projector-augmented plane wave (PAW)[56,57] ion-electron interaction as implemented in the Vienna ab initio Simulation Package (VASP).[58] The generalized gradient approximation (GGA) with the PW91 functional[59] and a 480 eV cutoff for the plane-wave basis set were adopted in all computations. The Brillouin zone was sampled with 1 × 1 × 1 and 1 × 1 × 12 Γ centered k point grid for the clusters and the 1D nanowire, respectively. Our supercells are large enough to ensure that the vacuum space is at least 10 Å, which can safely avoid the interaction between two sandwich clusters (nanowires). The convergence threshold was set as 10^{-4} eV in energy and 10^{-3} eV/Å in force. The positions of all the atoms in the supercell were fully relaxed during the geometry optimizations.

It is well known that DFT-GGA computations underestimate the on-site correlation effects of 3d TM atoms, which are important for the prediction of magnetic ordering. Therefore, we also performed some test computations by using the GGA+U method, and the results obtained from two methods are qualitatively the same. Moreover, since the GGA method tends to overestimate the exchange interaction, we also carried out some test computations within the local density approximation (LDA) using the Ceperley−Alder (CA) functional.[60] It is found that the LDA results agree qualitatively with the GGA ones.

3. RESULTS AND DISCUSSION

3.1. Structural Properties of $V_{n-1}Np_n$ SWCs. First, we examined the structural properties of VNp_2 SWC, the smallest $V_{n-1}Np_n$ SWC. Previously, it was proposed that $TMNp_2$ complexes adopt two geometries: the C_{2v} structure with both Np rings eclipsed, or the C_{2h} structure with two antiparallel Np rings.[61] However, our DFT computations revealed that both the C_{2v} and the C_{2h} isomers are not local minima of VNp_2 SWC, but a transition state, as characterized by frequency analysis (with only one imaginary frequency). To get the ground-state structure of VNp_2 SWC, we plotted the potential energy profile for Np ring rotation (Figure 1a), and found that the lowest energy structure of VNp_2 SWC shows C_2 symmetry with a rotation angle of 45° (Figure 1b), which is 80 and 139 meV lower in energy than the C_{2v} and C_{2h} isomer, respectively. This C_2 structure is a true local minimum, as confirmed by frequency analysis (without any imaginary frequency).

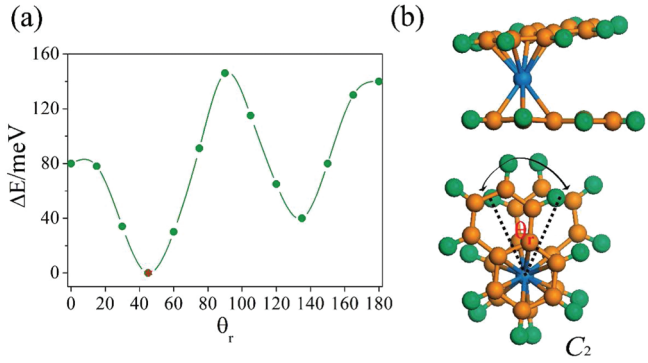

Figure 1. (a) Potential energy profile for the rotation of Np ring of VNp_2 SWC. (b) Ground state structure for VNp_2; both side (upper) and top (bottom) views are given. On the top view, we give a schematic representation of rotation angle θ_r, which is defined by the angle between two Np rings derived from the C_{2v} isomer. The brown, green, and blue balls denote C, H, and V atoms, respectively.

The ground state structure of VNp_2 SWC reminds us of the previous studies on the dimer structure of benzene[62−64] and naphthalene,[65−67] whose ground state structures have neither parallel nor antiparallel arrangement. For VNp_2 SWC, there are two competitive interactions between two free carbon hexagons: the attractive dispersion interaction and the repulsive electrostatic interaction. The C_{2v} isomer has the strongest dispersion interaction and the strongest electrostatic interaction, while the C_{2h} isomer has the weakest dispersion interaction and the weakest electrostatic interaction. It is the compromise between these two kinds of interactions that determines the ground state structure of VNp_2 SWC.

Adding a V atom and a Np ring to the as-synthesized VNp_2 SWC leads to V_2Np_3 SWC. Two types of V_2Np_3 SWC can be obtained by using different alignment patterns of V atoms: two V atoms bind to the same carbon hexagon in two sides (type-I, Figure 2a); or each V atom binds to a different carbon hexagon (type-II, Figure 2b).

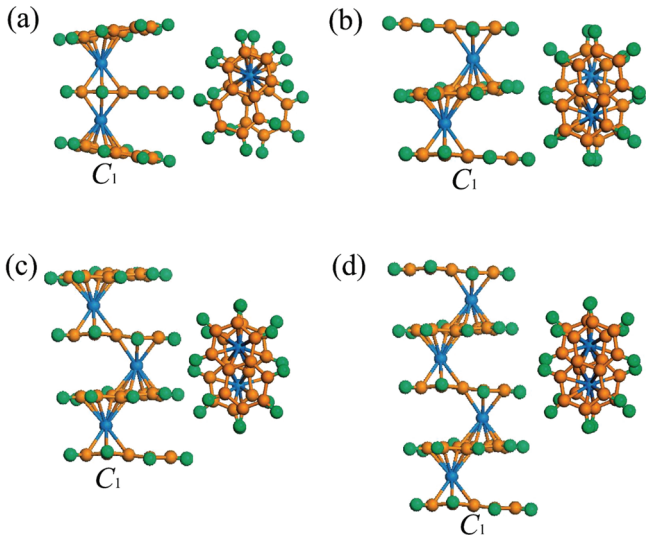

Figure 2. Side (left) and top (right) views of ground state structures of (a) type-I V_2Np_3, (b) type-II V_2Np_3, (c) V_3Np_4, and (d) V_4Np_5 SWC. All four SWCs have a C_1 symmetry.

To determine the ground state structure, we plotted the potential energy profiles of these two types of V_2Np_3 SWC

dx.doi.org/10.1021/jp2099398 | J. Phys. Chem. A 2012, 116, 1648−1654

(see Supporting Information) by rotating the added Np rings (the left two Np rings keep the rotation angle of 45°). It is found that type-I V_2Np_3 SWCs are much less stable than the type-II analogues. Obviously, binding two V atoms to the same carbon hexagon from different sides could result in a Coulomb repulsion between two V atoms. Moreover, the V−V distance in type-I V_2Np_3 SWC (3.49 Å) is much shorter than that of type-II V_2Np_3 SWC (4.30 Å). Thus, the reduced steric repulsion between two V atoms in type-II V_2Np_3 SWC should also contribute to the enhanced stability. In the most stable type-II structure of V_2Np_3 SWC (Figure 2b), the newly added Np ring also forms a rotation angle of 45° with its nearest Np ring and is parallel to its second-nearest Np ring. The additional frequency computation confirmed that this ground state structure of type-II V_2Np_3 SWC is also a local minimum (with no imaginary frequency).

To deduce the growth mechanism of $V_{n-1}Np_n$ SWCs, we also carefully studied the structural properties of V_3Np_4 and V_4Np_5 SWCs, which have been detected experimentally. For these two SWCs, we only considered the structures in which each V atom binds to two different carbon hexagons. By using the same searching method as mentioned above for V_2Np_3 SWC, we plotted the potential energy profiles of V_3Np_4 and V_4Np_5 SWCs for the rotation of the newly added Np rings to determine the ground state structures (see Supporting Information). In the energetically most favorable structures of these two SWCs (Figure 2c), the two nearest-neighbor Np rings also form a rotation angle of 45°, and two second-nearest-neighbor Np rings are parallel to each other.

The above results indicate that all the experimentally detected $V_{n-1}Np_n$ SWCs actually follow the same growth pattern. Note that in early years, Katz and co-workers[68] made different attempts to synthesize polymers in which TM atoms align in a zigzag shape; however, they did not succeed. Kurikawa et al.[5] successfully synthesized $V_{n-1}Np_n$ SWCs with this topology, but the intriguing structural properties of this complex have not been determined until now.

In the process of searching the ground state structures of $V_{n-1}Np_n$ SWCs, we found that the energy changes induced by rotating Np rings are rather low (<0.2 eV). This implies that Np rings of $V_{n-1}Np_n$ SWCs can rotate easily at room temperature, which may be an advantage for their potential applications. However, in this work, we do not consider the rotation effects of Np rings and only choose the most stable isomer to study the electronic and magnetic properties. The rotation of Np rings only brings a negligible change to the distance of two nearest-neighbor V atoms and is not expected to have a pronounced effect on the electronic and magnetic properties of $V_{n-1}Np_n$ SWCs.

3.2. Stability of $V_{n-1}Np_n$ SWCs. The above understanding of the structural properties of $V_{n-1}Np_n$ SWCs makes it feasible for us to rationalize why the peaks of $V_{n-1}Np_n$ SWCs s are more pronounced than those of $V_{2n-2}Np_n$ SWCs in the mass spectrum.[5] The stability comparison between these two types of SWCs may provide some insights. To estimate the stability, we have computed the binding energies per V atom for a series of $V_{n-1}Np_n$SWCs, and compared them with those of a series of $V_{2n-2}Np_n$ SWCs. For a V_mNp_n SWC, the binding energy, E_b, is defined according to the following equation:

$$E_b = mE_V + nE_{Np} - E_{V_mNp_n}$$

where E_V, E_{Np}, and $E_{V_mNp_n}$ are respective total energies of V atom, Np ring, and V_mNp_n SWCs. m and n are the number of V atoms and Np rings, respectively. According to our definition, those with larger binding energies are more stable. For these $V_{n-1}Np_n$ SWCs with $n > 5$, we adopted the same structures as determined above. The computed binding energies of examined V_mNp_n SWCs are summarized in Figure 3 as a function of the number of V atoms.

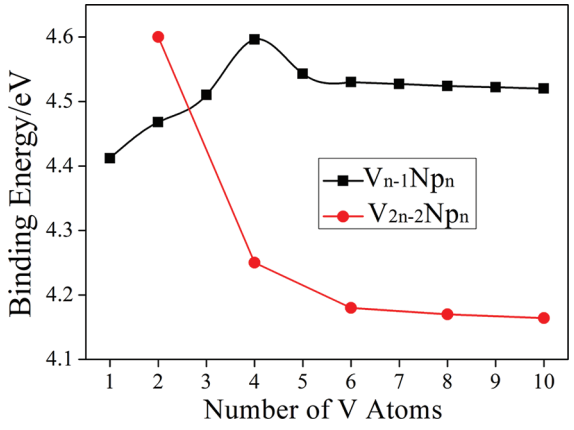

Figure 3. Binding energy of $V_{n-1}Np_n$ and $V_{2n-2}Np_n$ SWCs as a function of the number of V atoms.

The binding energies of $V_{n-1}Np_n$ SWCs first increase until the number of V atoms reaches 4, and then decrease as the size increases and gradually converge to 4.52 eV per V atom. In contrast, the binding energies of $V_{2n-2}Np_n$ SWCs decrease monotonically with increasing the number of V atoms and gradually converge to 4.17 eV per V atom. Note that the binding energy of V_2Np_2 SWC (4.61 eV per V atom) is even higher than those of all the $V_{n-1}Np_n$ SWCs examined here. The enhanced stability of V_2Np_2 SWC should be attributed to the formation of a weak bond between two V atoms, as revealed by Zhang et al.[43] However, the binding energies of multidecked $V_{2n-2}Np_n$ SWCs are much lower than those of $V_{n-1}Np_n$ SWCs. The lower binding energies of multidecked $V_{2n-2}Np_n$ SWCs should be due to the repulsive Coulomb interaction between V atoms at two sides of carbon hexagons.

The binding energies essentially reflect the order of the stability and to some extent the synthesis difficulty. Our results could explain why the peaks of $V_{n-1}Np_n$ SWCs are more pronounced than those of multidecked $V_{2n-2}Np_n$ SWCs, and V_2Np_2 SWC has a rather pronounced peak in the mass spectrum. However, the binding energy of VNp_2 SWC (4.41 eV) is lower than those of the other experimentally observed multidecked $V_{n-1}Np_n$ SWCs (n = 3, 4, 5) and V_2Np_2 SWC. Why is the peak of VNp_2 SWC most pronounced in the mass spectrum? It may be due to the fact that the growth of SWCs is not only determined simply by the thermodynamic stability, but also controlled by some complicated kinetic factors.

3.3. Electronic and Magnetic Properties of $V_{n-1}Np_n$ SWCs. We have systematically studied the electronic and magnetic properties of $V_{n-1}Np_n$ SWCs based on their ground state structures. The main results concerning the electronic and magnetic properties of $V_{n-1}Np_n$ SWCs are summarized in Table 1, including the ground magnetic state, the energy difference between ferromagnetic (FM) and antiferromagnetic (AFM) states ($\Delta E_{FM\text{-}AFM}$, $\Delta E_{FM\text{-}AFM} = E_{FM} - E_{AFM}$), the total magnetic moments, and the highest occupied molecular orbital (HOMO)−lowest unoccupied molecular orbital (LUMO) gaps for the majority and minority spin.

dx.doi.org/10.1021/jp2099398 | J. Phys. Chem. A 2012, 116, 1648−1654

Table 1. Ground Magnetic State (GMS), Energy Difference between FM and AFM States (ΔE_{FM-AFM}), Total Magnetic Moments (TMM), and HOMO−LUMO Gap for a Series of $V_{n-1}Np_n$ SWCs ($2 \leq n \leq 5$)

				HOMO−LUMO (eV)	
SWC	GMS	ΔE_{FM-AFM} (meV)	TMM (μB)	majority	minority
VNp_2	FM (↑)		1	1.28	1.16
V_2Np_3	AFM (↑↓)	31	0	1.22	1.22
V_3Np_4	AFM (↑↓↑)	55	1	1.21	1.12
V_4Np_5	AFM (↑↓↓↑)	72	0	1.13	1.13

In VNp_2 SWC, each Np ring has 10 valence electrons, forming a stable aromatic configuration with $4m + 2$ (where m is an integer). There is only 0.08 lel charge transfer from V atom to Np rings according to the Bader population analysis. VNp_2 SWC has a magnetic ground state, which is 190 meV lower in energy than the nonmagnetic state. According to the crystal field theory, the TM 3d oribitals could split into three parts in the crystal field of a carbon hexagon: a 2-fold degenerated bonding orbital mainly from d_{xy} and $d_{x^2-y^2}$, a 2-fold degenerated antibonding orbital contributed by d_{xz} and d_{yz} oribitals, and a nonbonding oribtal with d_{z^2} character. As seen from the computed local density of states (LDOS), V atom uses three of its five valence electrons (two 4s electrons fill the 3d orbitals) to fill three majority orbitals (d_{xy}, $d_{x^2-y^2}$, and d_{z^2}), and the left two valence electrons fill two minority (d_{xy}, $d_{x^2-y^2}$) orbitals, resulting in one unpaired electron to d_{z^2} oribital. Therefore, the total magnetic moment of VNp_2 SWC is 1 μB, which equals that of VBz_2 SWC.[24] The localized magnetic moment of the V atom is 1.11 μB, and the Np ring also has a small local magnetic moment of −0.06 μB. Since VNp_2 SWC has a spin-polarized ground state, its HOMO−LUMO gaps for the majority and minority spin are not equivalent: 1.28 and 1.16 eV for majority and minority spin, respectively.

However, the local magnetic moment cannot guarantee the collective magnetism. For V_2Np_3 SWC, we considered two spin-polarized states to determine the ground state: the AFM state with opposite spin orientation between two V atoms, and the FM state with same spin orientation between two V atoms. Our computations showed that the AFM state is 31 meV lower in energy than the FM state. Hence, V_2Np_3SWC should have an AFM ground state, and the total magnetic moment is zero. The local magnetic moments for two V atoms are 1.10 and −1.10 μB, respectively. The upper and bottom Np rings have a −0.06 and 0.06 μB local magnetic moment, respectively. Interestingly, for the middle Np ring, the spin orientations are opposite for two carbon hexagons, thus resulting in a zero local magnetic moment.

Why are the local magnetic moments in V_2Np_3 SWC antiferromagnetically coupled, while they are ferromagnetically coupled in V_2Bz_3 SWC?[24] Two mechanisms have been proposed to explain the ferromagnetism in SWCs and SWNs, namely, the double-exchange (DE) mechanism, which involves the direct spin exchange interaction between neighboring TM atoms, and the charge-transfer (CT) based mechanism, which involves indirect spin exchange interaction between TM atoms. For example, it was suggested that ferromagnetism in Bz-based SWCs and SWNs is due to the DE mechanism,[30] while that in Cp-based SWCs and SWNs is due to the CT mechanism.[37] For V_2Np_3 SWC, CT mechanism is obviously not available due to the near neutral feature of Np rings and V atoms. As shown in Figure 4b, a considerable gap appears in the 3d states of V_2Np_3

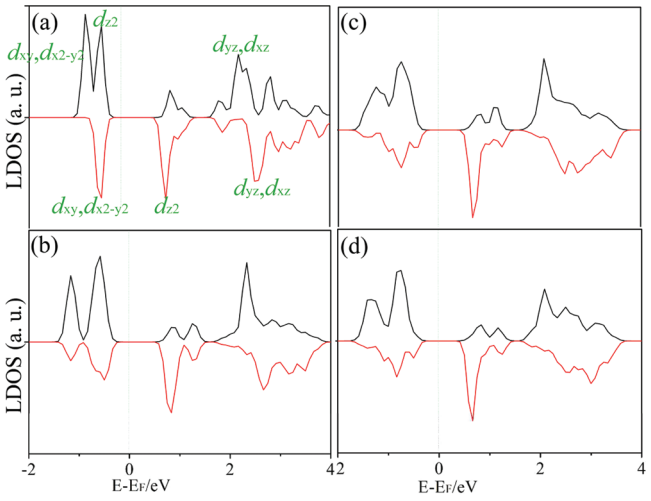

Figure 4. Local density of states for 3d orbitals of V atom in (a) VNp_2, (b) V_2Np_3, (c) V_3Np_4, and (d) V_4Np_5 SWC, respectively. The black and red lines denoted majority and minority states, respectively.

SWC since no 3d orbital is partially filled, which makes the direct spin exchange coupling of local magnetic moments less effective, and the DE mechanism is hence not effective. Therefore, two V atoms of the V_2Np_3 cluster should adopt the AFM coupling due to the superexchange mechanism.

For V_3Np_4 SWC, the FM state and two kinds of AFM states (AFM1-↑↓↑, and AFM2-↑↑↓) were considered. The AFM1 state is the ground state, which is 30 and 55 meV lower in energy than the AFM2 and FM states, respectively. The total magnetic moment of V_3Np_4 SWC state is 1 μB, which equals that of VNp_2 SWC. The upper, middle, and bottom V atoms have a 1.11, −1.10, 1.11 μB local magnetic moment, respectively. The magnetizations for upper and bottom Np rings are both −0.06 μB, while the local magnetic moments for the two middle Np rings are 0. The AFM coupling of local magnetic moments in V_3Np_4 SWC should also be essentially attributed to the presence of the gap in 3d states of V atoms (Figure 3c).

When the number of V atoms increases to 4, the situation becomes more complicated since there are many possible coupling patterns between local magnetic moments. We have computed the total energies of the FM state (↑↑↑↑) and 5 AFM states (AFM1-↑↓↑↓, AFM2-↑↑↓↓, AFM3-↑↓↓↑, AFM4-↑↑↓↑, and AFM5-↑↑↑↓) to determine the ground state of V_4Np_5 SWC. The FM state is of the highest energy, while the AFM1 state is the most favorable energetically. It means that in V_4Np_5 SWC, the two nearest-neighbor V atoms are antiferromagnetically coupled, while the two second-nearest-neighbor V atoms have the same spin direction. From upper to bottom, the four V atoms of V_4Np_5 SWC have a local magnetic moment of 1.10, −1.09, 1.09, and −1.10 μB, respectively, resulting in a total magnetic moment of 0 μB, the same as V_2Np_3 SWC.

From the above, we can conclude that due to the presence of gaps in 3d orbitals, V atoms in $V_{n-1}Np_n$ SWCs favor AFM coupling via the superexchange mechanism. Thus, when n is odd, $V_{n-1}Np_n$ SWCs should have a total magnetic moment of 1 μB; when n is even, the total magnetic moment of $V_{n-1}Np_n$ SWCs should be 0.

dx.doi.org/10.1021/jp2099398 | J. Phys. Chem. A 2012, 116, 1648−1654

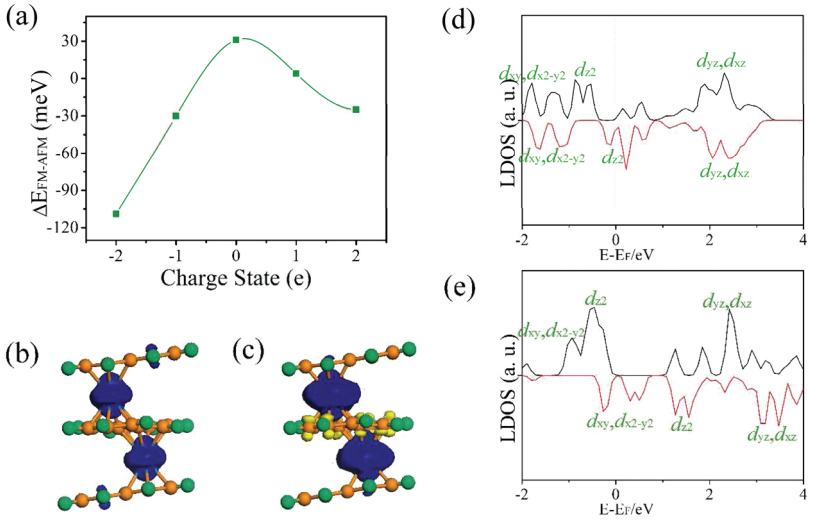

Figure 5. (a) Energy difference between the FM and AFM states (ΔE_{FM-AFM}) as a function of the charge state for V_2Np_3 SWC. (b,c) Spin densities for V_2Np_3 SWC at the charge state of −2 and +2, respectively. The isosurface value is 0.05 e/au. (d,e) Local density of states of 3d states for V_2Np_3 SWC at the charge state of −2 and +2, respectively.

3.4. Effects of Electron and Hole Injection on Magnetic Properties of $V_{n-1}Np_n$ SWCs. Recently, Atodiresei et al.[39] have reported that it is possible to manipulate the magnetization direction in $Eu_2(COT)_3$ SWC by changing their oxidation state. Zhang et al.[43] demonstrated that antiferromagnetic ordering of local magnetic moments in V_2Np SWN and $V_{2n-2}Np_n$ SWCs can be switched to ferromagnetic ordering by electron injection. Since the AFM coupling of V atoms in the V_mNp_n SWCs is due to the presence of gap in d states, the injection of electrons or holes may eliminate the gap and then make the FM coupling favorable. Thus, we studied the effects of electron and hole injection on the magnetic properties of VNp clusters. V_2Np_3 SWC was chosen as an example. In Figure 5a, we present the energy difference between the FM and the AFM states of V_2Np_3 SWC as a function of charge state.

Injecting one electron is sufficient to switch the magnetic ordering of V_2Np_3 SWC: the FM state is 30 meV lower in energy than the AFM state; injecting two electrons can further stabilize the FM state, and the resulting ΔE_{FM-AFM} (−109 meV) is adequate for preserving the robust room-temperature ferromagnetism. Especially, the electron injection significantly decreases the local magnetic moments on V atoms. For example, two V atoms both have a local magnetic moment of 0.65 μB at the −2 charge state (Figure 5b). Similar phenomenon was found in $V_{2n-2}Np_n$ SWCs by Zhang et al.[43]

Injecting holes into V_2Np_3 SWC can also switch the magnetic coupling from AFM to FM: when two holes are injected, the FM state is 25 meV lower in energy than the AFM state. However, injecting only one hole is not sufficient: though stabilized by the hole injection, the FM state is still 2 meV higher in energy than the AFM state in the +1 charge state. In contrast to electron injection, hole injection significantly increases the local magnetic moments of V atoms. For example, at the +2 charge state, the magnetizations of two V atom have been increased to 1.78 μB (Figure 5c).

To understand the switch mechanism, we computed the LDOS for 3d orbitals of V atoms in V_2Np_3 SWC at −2 and +2 charge states. Because of the electron injection, the minority d_{z^2} orbital changes from unoccupied to partially occupied (Figure 5d), which moves the gap of 3d states and facilitates the direct spin exchange. Thus, the local magnetic moments could adopt the FM coupling following the DE mechanism. Since the injected electrons mainly occupy the minority d_{z^2} oribital, the local magnetic moments are hence decreased. When two holes are injected, the d_{z^2} orbital is less influenced, but the minority d_{xy} and $d_{x^2-y^2}$ orbitals change from occupied to partially occupied (Figure 5e), which not only increases the local magnetic moments but also makes the DE mechanism effective.

3.5. Electronic and Magnetic Properties of the Infinite 1D VNp SWN. On the basis of the energetically preferred structural pattern of $V_{n-1}Np_n$ SWCs, we constructed the infinite 1D VNp SWN, and studied its electronic and magnetic properties. The unit cell of VNp SWN consists of two Np rings and two V atoms (Figure 6a).

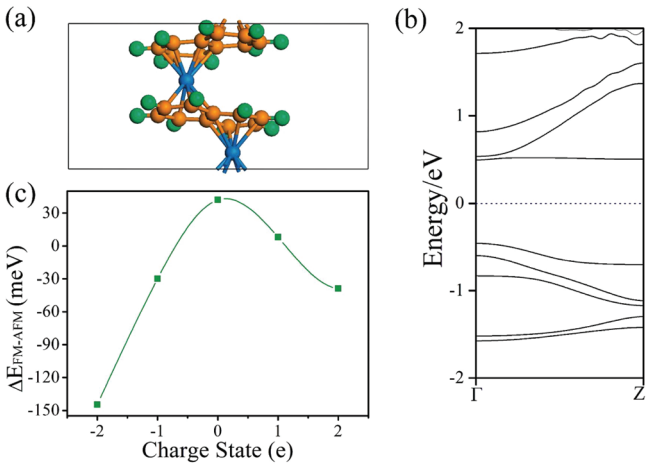

Figure 6. (a) Side view of geometric structure and (b) band structure of VNp SWN. The blue dashed line in panel b denotes the position of Fermi level. (c) Energy difference between the FM and AFM states ($E_{FM} - E_{AFM}$) as a function of charge state for VNp SWN.

VNp SWN has an AFM ground state, which is 58 meV lower in energy than the FM state. In the AFM ground state, the optimized lattice constant is 7.27 Å, and the binding energy (4.52 eV per V atom) of VNp SWN is 0.35 eV higher than that of V_2Np SWN at the same theoretical level. The 1.12 and

dx.doi.org/10.1021/jp2099398 | J. Phys. Chem. A 2012, 116, 1648−1654

−1.12 μB local magnetic moment of the two V atoms in an AFM state unit cell diminishes the total magnetic moment. As a result, VNp SWN presents symmetrical majority and minority bands, and both spin channels have a 1.10 eV band gap (Figure 6b).

The unique structural properties of VNp SWN remind us of the possible existence of Peierls deformation, which can happen in a 1D system if a partially filled energy band crosses the Fermi level at the wave-vector $k = \pi/2c$ (c is the lattice constant). At the low temperature, this partially filled energy band is rather unstable due to the strong electron−phonon coupling, which could result in structural deformation along the axial direction. To test the existence of Peierls instability in our VNp SWNs, we performed the DFT computations for a VNp SWN with a rotation angle of 0°. In contrast to the AFM ground state in the most stable configuration (θ_r = 45°), the ground state of this VNp SWN is FM, which is 76 meV lower in energy than the AFM state. Especially, a half-filled majority band crosses the Fermi level near the midpoints of the symmetry line of ΓZ, which is vigorous evidence for the existence of Peierls instability (Figure S2, Supporting Information). VNp SWN with a rotation angle of 45° is 400 eV lower in energy than VNp SWN with a rotation angle of 0°. This energy gain should essentially result from the electronic contribution owing to the band gap opening at the Fermi level. We noted that the V−V distance in the VNp nanowire with a rotation angle of 45° is 4.27 Å, much shorter than the corresponding value of 4.38 Å in the VNp nanowire with a rotation angle of 0°. The contraction of V−V distance in the VNp with 45° rotation angle would enhance the stability of VNp nanowire and is evidence for the occurrence of Peierls deformation. Moreover, the type-II V_2Np_3 SWC with a rotation angle equal to 0° also has a FM ground state, which is 98 meV lower in energy than the AFM state. Therefore, the AFM coupling and the adoption of 45° rotation angle in VNp SWN and $V_{n-1}Np_n$ SWCs is a result of Peierls deformation.

Similarly, the coupling of local magnetic moments in the VNp SWN can be tuned by electron or hole injection. Injecting one electron per unit cell is sufficient to tune VNp SWN from AFM coupling to FM coupling: the FM state is 40 meV lower in energy than the AFM state (Figure 6c). The FM state can be further stabilized at the −2 charge state. Similar to V_2Np_3 SWC, though injecting one hole can stabilize the FM state, but it is not sufficient to tune VNp SWN into FM coupling. Injecting one more hole is capable to switch the magnetic ordering of VNp SWN, and at this charge state (+2), the FM state is 39 meV lower in energy than the AFM state.

4. CONCLUSIONS

In summary, we have systematically investigated the structural, energetic, electronic, and magnetic properties of $V_{n-1}Np_n$ SWCs by means of density functional theory computations. All $V_{n-1}Np_n$ SWCs studied in this work follow the same growth pattern: the two nearest-neighboring Np rings form a rotation angle of 45°, the two second-nearest-neighboring Np rings are parallel to each other, and the V atoms align in a zigzag chain. The computed binding energies indicate that $V_{n-1}Np_n$ SWCs are more stable than the multidecked $V_{2n-2}Np_n$ SWCs, while V_2Np_2 SWC has the largest binding energy among these V_mNp_n SWCs, which is in line with the abundance observed in the mass spectroscopy. $V_{n-1}Np_n$ SWCs are all semiconducting with a 1.1−1.3 eV HOMO−LUMO gap. The local magnetic moments in $V_{n-1}Np_n$ SWCs favor AFM coupling via the superexchange mechanism, and $V_{n-1}Np_n$ SWCs have a total magnetic moment of 1 and 0 μB when n is even and odd, respectively. Especially, we demonstrated that the electron or hole injection can tune the magnetic ordering in $V_{n-1}Np_n$ SWCs and VNp SWN, leading to the more favorable FM coupling via the double exchange mechanism. The electron injection decreases the local magnetic moments, while the hole injection increases the local magnetic moments. Moreover, the AFM coupling and unique structural properties of $V_{n-1}Np_n$ SWCs and VNp SWN is a result of Peierls deformation. With such interesting electronic and magnetic properties, $V_{n-1}Np_n$ SWCs are expected to have potential applications in nanoelectronics and spintronics.

■ ASSOCIATED CONTENT

Supporting Information

Potential energy profiles for V_2Np_3, V_3Np_4 and V_4Np_5 SWCs and geometric structure and spin-polarized electronic band structure of VNp sandwich nanowire with a rotation angle of 0°. This material is available free of charge via the Internet at http://pubs.acs.org.

■ AUTHOR INFORMATION

Corresponding Author

*E-mail: zhouzhen@nankai.edu.cn (Z.Z.); zhongfangchen@gmail.com (Z.C.).

Notes

The authors declare no competing financial interest.

■ ACKNOWLEDGMENTS

Support in U.S.A. by NSF Grant EPS-1010094 and in China by MOE NCET (08-0293) and Innovation Team (IRT0927), is gratefully acknowledged. This work was also supported in part by the National Science Foundation through TeraGrid resources, and the computations were partly performed on TianHe-1(A) at the National Supercomputer Center in Tianjin.

■ REFERENCES

(1) Kealy, T. J.; Pauson, P. L. *Nature* **1951**, *168*, 1039−1040.
(2) Long, N. J. In *Metallocenes: An Introduction to Sandwich Complexes*; Blackwell Science: Oxford, U.K., 1998.
(3) Hoshino, K.; Kurikawa, T.; Takeda, H.; Nakajima, A.; Kaya, K. *J. Phys. Chem.* **1995**, *99*, 3053−3055.
(4) Weis, P.; Kemper, P. R.; Bowers, M. T. *J. Phys. Chem. A* **1997**, *101*, 8207−8213.
(5) Kurikawa, T.; Takeda, H.; Hirano, M.; Judai, K.; Arita, T.; Nagao, S.; Nakajima, A.; Kaya, K. *Organometallics* **1999**, *18*, 1430−1438.
(6) Kurikawa, T.; Negishi, Y.; Satoshi, F. H.; Nagao, S.; Miyajima, K.; Nakajima, A.; Kaya, K. *J. Am. Chem. Soc.* **1998**, *120*, 11766−11772.
(7) Nakajima, A.; Kaya, K. *J. Phys. Chem. A* **2000**, *104*, 176−191.
(8) Nagao, S.; Kato, A.; Nakajima, A. *J. Am. Chem. Soc.* **2000**, *122*, 4221−4222.
(9) Miyajima, K.; Nakajima, A.; Yabushita, S.; Knickelbein, M. B.; Kaya, K. *J. Am. Chem. Soc.* **2004**, *126*, 13202−13203.
(10) Miyajima, K.; Knickelbein, M. B.; Nakajima, A. *Polyhedron* **2005**, *24*, 2341−2345.
(11) Hosoya, N.; Takegami, R.; Suzumura, J.; Yada, K.; Koyasu, K.; Miyajima, K.; Mitsul, M.; Knickelbein, M. B.; Yabushita, S.; Nakajima, A. *J. Phys. Chem. A* **2005**, *109*, 9−12.
(12) Takegami, R.; Hosoya, N.; Suzumura, J.; Yada, K.; Nakajima, A.; Yabushita, A. *Chem. Phys. Lett.* **2005**, *403*, 169−174.
(13) Takegami, R.; Hosoya, N.; Suzumura, J.; Nakajima, A.; Yabushita, S. *J. Phys. Chem. A* **2005**, *109*, 2476−2486.
(14) Scott, A. C.; Foster, N. R.; Grieves, G. A.; Duncan, M. A. *Int. J. Mass. Spec.* **2007**, *263*, 171−178.

(15) Miyajima, K.; Yabushita, S.; Knickelbein, M. B.; Nakajima, A. *J. Am. Chem. Soc.* **2007**, *129*, 8473−8480.
(16) Miyajima, K.; Knickelbein, M. B.; Nakajima, A. *J. Phys. Chem. A* **2008**, *112*, 366−375.
(17) Ashley, A. E.; Cooper, R. T.; Wildgoose, G. G.; Green, J. C.; O'Hare, D. *J. Am. Chem. Soc.* **2008**, *130*, 15662.
(18) Zheng, W. J.; Nilles, J. M.; Thomas, O. C.; Bowen, K. H. Jr. *Chem. Phys. Lett.* **2005**, *401*, 266−270.
(19) Li, J.; Bursten, E. *J. Am. Chem. Soc.* **1998**, *120*, 11456−11466.
(20) Liu, W. J.; Dolg, M.; Fulde, P. *Inorg. Chem.* **1998**, *37*, 1067−1072.
(21) Pandey, R.; Rao, B. K.; Jena, P.; Newsam, J. M. *Chem. Phys. Lett.* **2000**, *321*, 142−150.
(22) Pandey, R.; Rao, B. K.; Jena, P.; Blanco, M. A. *J. Am. Chem. Soc.* **2001**, *123*, 3799−3808.
(23) Kandalam, A. K.; Rao, B. K.; Jena, P.; Pandey, R. *J. Chem. Phys.* **2004**, *120*, 10414.
(24) Wang, J.; Acioli, P. H.; Jellinek, J. *J. Am. Chem. Soc.* **2005**, *127*, 2812−2813.
(25) Wang, J.; Jellinek, J. *J. Phys. Chem. A* **2005**, *109*, 10180−10182.
(26) Rahman, M. M.; Kasai, H.; Dy, E. S. *Jpn. J. Appl. Phys.* **2005**, *44*, 7954−7956.
(27) Kang, H. S. *J. Phys. Chem. A* **2005**, *109*, 9292−9298.
(28) Kang, H. S. *J. Phys. Chem. A* **2005**, *109*, 478−483.
(29) Kua, J.; Tomlin, K. M. *J. Phys. Chem. A* **2006**, *110*, 11988−11994.
(30) Xiang, H. J.; Yang, J. L.; Hou, J. G.; Zhu, Q. S. *J. Am. Chem. Soc.* **2006**, *128*, 2310−2314.
(31) Maslyuk, V. V.; Bagrets, A.; Meded, V.; Arnold, A.; Evers, F.; Brandbyge, M.; Bredow, T.; Mertig, I. *Phys. Rev. Lett.* **2006**, *97*, 097201.
(32) Koleini, M.; Paulsson, M.; Brandbyge, M. *Phys. Rev. Lett.* **2006**, *98*, 197202.
(33) Mokrousov, Y.; Atodiresei, N.; Bihlmayer, G.; Gel, S.; Blugel, S. *Nanotechnology* **2007**, *18*, 495402.
(34) Weng, H. M.; Ozaki, T.; Terakura, K. *J. Phys. Soc. Jpn.* **2008**, *77*, 014301.
(35) Mallajosyula, S. S.; Pati, S. K. *J. Phys. Chem. B* **2008**, *111*, 13877−13880.
(36) Zhou, L.; Yang, S.; Ng, M.; Sullivan, M. B.; Tan, V. B. C.; Shen, L. *J. Am. Chem. Soc.* **2008**, *130*, 4023−4027.
(37) Shen, L.; Yang, S.-W.; Ng, M.-F.; Ligatchev, V.; Zhou, L.; Feng, Y. *J. Am. Chem. Soc.* **2008**, *130*, 13956−13960.
(38) Wang, L.; Cai, Z.; Wang, J.; Lu, J.; Luo, G.; Lai, L.; Zhou, J.; Qin, R.; Gao, Z.; Yu, D.; et al. *Nano Lett.* **2008**, *8*, 3640−3644.
(39) Atodiresei, N.; Dederichs, P. H.; Mokrousov, Y.; Bergqvist, L.; Bihlmayer, G.; Blügel, S. *Phys. Rev. Lett.* **2008**, *100*, 117207.
(40) Zhang, X. Y.; Wang, J. L.; Gao, Y.; Zeng, X. C. *ACS Nano* **2009**, *3*, 537−545.
(41) Zhang, X. Y.; Ng, M. F.; Wang, Y. B.; Wang, J. L.; Yang, S. W. *ACS Nano* **2009**, *3*, 2515−2522.
(42) Wu, X. J.; Zeng, X. C. *J. Am. Chem. Soc.* **2009**, *131*, 2310−2314.
(43) Zhang, Z. H.; Wu, X. J.; Guo, W. L.; Zeng, X. C. *J. Am. Chem. Soc.* **2009**, *132*, 10215−10217.
(44) Dai, H. X.; Jin, H. M.; Yang, S. W.; Lim, K. H. *J. Phys. Chem. C* **2009**, *113*, 21422−21427.
(45) Dai, H. X.; Jin, H. M.; Lim, K. H.; Yang, S. W. *J. Phys. Chem. C* **2010**, *114*, 21705−21707.
(46) Shen, L.; Jin, H. M.; Ligatchev, V.; Yang, S. W.; Sullivan, M. B.; Feng, Y. P. *Phys. Chem. Chem. Phys.* **2010**, *12*, 4555−4559.
(47) Zhang, X. Y.; Wang, J. L. *J. Phys. Chem. A* **2010**, *114*, 21893−21899.
(48) Huang, J.; Li, Q. X.; Xu, K.; Su, H. B.; Yang, J. L. *J. Phys. Chem. C* **2010**, *114*, 11946−11950.
(49) Zhang, X. Y.; Tian, Z.; Yang, S. W.; Wang, J. L. *J. Phys. Chem. C* **2010**, *115*, 2948−2953.
(50) Li, Y. C.; Zhou, G.; Li, J.; Wu, J.; Gu, B. L.; Duan, W. H. *J. Phys. Chem. C* **2011**, *115*, 7292−7297.
(51) Wu, M. H.; Zeng, X. C. *Appl. Phys. Lett.* **2011**, *99*, 053121.
(52) Elschenbroich, C.; Möckel, R. *Angew. Chem., Int. Ed.* **1977**, *16*, 870−871.
(53) Ellis, J. E.; Blackburn, D. W.; Yuen, P.; Jang, M. *J. Am. Chem. Soc.* **1993**, *115*, 11616−11617.
(54) Pomije, M. K.; Kurth, C. J.; Ellis, J. E.; Barybin, M. V. *Organometallics* **1997**, *16*, 3582−3587.
(55) Elschenbroich, C.; Möckel, R.; Vasilkov, A.; Metz, B.; Harms, K. *Eur. J. Inorg. Chem.* **1998**, *1998*, 1391−1401.
(56) Blöchl, P. E. Projector Augmented-Wave Method. *Phys. Rev. B* **1994**, *50*, 17953−17979.
(57) Kresse, G.; Joubert, D. *Phys. Rev. B* **1999**, *59*, 1758−1775.
(58) Kresse, G.; Hafner, J. *Phys. Rev. B* **1993**, *47*, 558−561.
(59) Perdew, J. P.; Wang, Y. *Phys. Rev. B* **1992**, *45*, 13244−13249.
(60) Ceperley, D. M.; Alder, B. J. *Phys. Rev. Lett.* **1980**, *45*, 566−569.
(61) Osborne, J. H.; Trogler, W. C.; Morand, P. D.; Francis, C. G. *Organometallics* **1987**, *6*, 94−100.
(62) Hobza, P.; Selzle, H. L.; Schlag, E. W. *J. Am. Chem. Soc.* **1994**, *116*, 3500−3506.
(63) Tsuzuki, S.; Honda, K.; Uchimaru, T.; Mikami, M.; Tanabe, K. *J. Am. Chem. Soc.* **2001**, *123*, 104−112.
(64) Sinnokrot, M. O.; Valeev, E. F.; Sherrill, C. D. *J. Am. Chem. Soc.* **2002**, *124*, 10887−10893.
(65) Walsh, T. R. *Chem. Phys. Lett.* **2002**, *363*, 45−51.
(66) Saeki, M.; Akagi, H.; Fujii, M. *J. Chem. Theory Comput.* **2006**, *2*, 1176−1183.
(67) Sato, T.; Tsuneda, T.; Hirao, K. *J. Chem. Phys.* **2005**, *123*, 104307.
(68) Katz, T. J.; Ślusarek, W. *J. Am. Chem. Soc.* **1980**, *102*, 1058−1063.